Voltage-gated sodium channel (Na_V) protein dissection creates a set of functional pore-only proteins

David Shaya[a], Mohamed Kreir[b], Rebecca A. Robbins[c], Stephanie Wong[a], Justus Hammon[a], Andrea Brüggemann[b], and Daniel L. Minor, Jr.[a,c,d,e,f,1]

[a]Cardiovascular Research Institute, [c]Departments of Biochemistry and Biophysics and [d]Cellular and Molecular Pharmacology, [e]California Institute for Quantitative Biomedical Research, University of California, San Francisco, CA 94158-9001; [f]Physical Biosciences Division, Lawrence Berkeley National Laboratory, Berkeley, CA 94720; and [b]Nanion Technologies GmbH, Gabrielenstrasse 9, D-80636 Munich, Germany

Edited by Richard W. Aldrich, University of Texas at Austin, Austin, TX, and approved June 14, 2011 (received for review April 30, 2011)

Many voltage-gated ion channel (VGIC) superfamily members contain six-transmembrane segments in which the first four form a voltage-sensing domain (VSD) and the last two form the pore domain (PD). Studies of potassium channels from the VGIC superfamily together with identification of voltage-sensor only proteins have suggested that the VSD and the PD can fold independently. Whether such transmembrane modularity is common to other VGIC superfamily members has remained untested. Here we show, using protein dissection, that the *Silicibacter pomeroyi* voltage-gated sodium channel (Na_VSp1) PD forms a stand-alone, ion selective pore (Na_VSp1p) that is tetrameric, α-helical, and that forms functional, sodium-selective channels when reconstituted into lipid bilayers. Mutation of the Na_VSp1p selectivity filter from LESWSM to LDDWSD, a change similar to that previously shown to alter ion selectivity of the bacterial sodium channel Na_VBh1 (NaChBac), creates a calcium-selective pore-only channel, Ca_VSp1p. We further show that production of PDs can be generalized by making pore-only proteins from two other extremophile Na_Vs: one from the hydrocarbon degrader *Alcanivorax borkumensis* (Na_VAb1p), and one from the arsenite oxidizer *Alkalilimnicola ehrlichei* (Na_VAe1p). Together, our data establish a family of active pore-only ion channels that should be excellent model systems for study of the factors that govern both sodium and calcium selectivity and permeability. Further, our findings suggest that similar dissection approaches may be applicable to a wide range of VGICs and, thus, serve as a means to simplify and accelerate biophysical, structural, and drug development efforts.

Voltage-gated sodium channels (Na_Vs) are large polytopic membrane proteins involved in action potential generation in excitable cells and belong to an ion channel superfamily that includes voltage-gated calcium channels (Ca_Vs), voltage-gated potassium channels (K_Vs), and transient receptor potential (TRP) channels (1, 2). Within the voltage-gated ion channel (VGIC) superfamily, Na_Vs and Ca_Vs are close relatives (1–3) that share a topology of 24 transmembrane segments organized in four homologous six-transmembrane repeats. These two families are also thought to share some common structure in the ion selectivity filter despite having markedly different ion permeation properties (4). Both are central to human neuromuscular, cardiovascular, and neural physiology. Consequently, they are targets for a host of pharmaceuticals used to treat a diverse set of disorders and remain active targets for drug development (5–7). Recently, single subunit, six-transmembrane segment Na_Vs have been identified in a large number of bacteria from diverse environments (8, 9). These channels show clear similarities to eukaryotic Na_Vs and Ca_Vs (2, 9, 10), suggesting that the prokaryotic channels may have been ancestors of the more complex vertebrate channels.

Despite the central importance of Na_Vs, nothing is known about the high-resolution structure of the Na_V transmembrane portions. Present knowledge is limited to low-resolution electron microscopy studies (19 Å) that have suggested some general features of Na_Vs purified from eel electric organs (11) but that lack the resolution for detailed mechanistic insight. Study of bacterial Na_Vs provides a simplified system for understanding basic aspects of both Na_V and Ca_V function and holds promise as a template for guiding small molecule modulator development (6). Although there have been ongoing efforts to produce bacterial Na_V samples that can be used for biochemical and structural studies (12–14), these have yet to achieve the multi-milli-gram amounts required for extensive structural studies.

Here, we show that a protein dissection approach produces folded, electrophysiologically active pore domains (PDs) from a set of bacterial Na_Vs. These PDs are well-behaved, biochemically tractable, stand-alone pores that can be produced in multi-milli-gram amounts. Application of a battery of biochemical and biophysical characterizations demonstrates that the PD-only proteins self-assemble as tetramers having α-helical structure and form functional channels when incorporated into lipid bilayers. We further show that introduction of aspartic acid residues at key selectivity filter positions in the *Silicibacter pomeroyi* PD-only channel Na_VSp1p creates a channel, Ca_VSp1p, in which ion selectivity is changed from sodium to calcium. Taken together, our data demonstrate that the Na_V pore-only proteins are active and biochemically accessible ion channels. Because of their favorable biochemical properties, these Na_V PDs should provide excellent model systems for the structural study of the factors that govern sodium selectivity and permeability. Further, the dissection strategy eliminates the potential complications that arise from voltage-sensing domain (VSD) conformational heterogeneity and should be a generally applicable means to simplify studies of the PDs of other VGIC superfamily members.

Results

Creation of a Pore-Only Na_V. We previously identified an Na_V from the marine sulfur-reducing bacterium *S. pomeroyi* (Na_VSp1), which is functional when expressed in mammalian cells (8), as a protein that could be highly expressed (approximately 20 mg L^{-1}) in *Escherichia coli* membranes (15). Despite the high expression level, size-exclusion chromatography analysis of purified, detergent-solubilized Na_VSp1 revealed a broad elution profile indicative of a polydisperse sample that was not well suited to further

Author contributions: D.S., M.K., and D.L.M. designed research; D.S., M.K., R.A.R., S.W., and J.H. performed research; D.S., M.K., R.A.R., S.W., and J.H. contributed new reagents/analytic tools; D.S., M.K., R.A.R., S.W., J.H., A.B., and D.L.M. analyzed data; and D.S., M.K., and D.L.M. wrote the paper.

The authors declare no conflict of interest.

This article is a PNAS Direct Submission.

Freely available online through the PNAS open access option.

[1]To whom correspondence should be addressed. E-mail: daniel.minor@ucsf.edu.

This article contains supporting information online at www.pnas.org/lookup/suppl/doi:10.1073/pnas.1106811108/-/DCSupplemental.

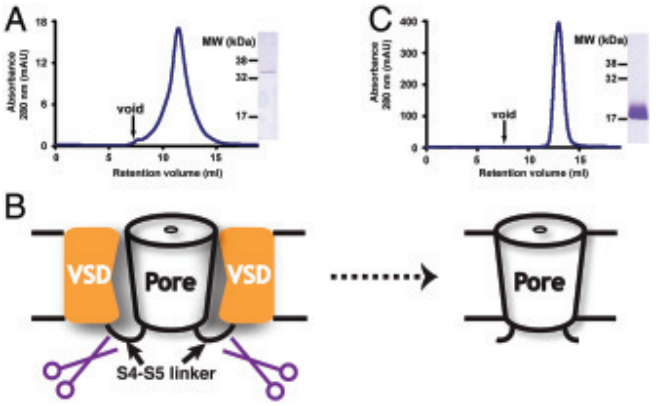

Fig. 1. Creation of a pore-only Na_V. (*A*) Superdex 200 size-exclusion chromatography of Na_VSp1 in 200 mM NaCl, 0.3 mM DDM, 20 mM HEPES, pH 8.0. (*Inset*) Fifteen percent SDS-PAGE of the peak fraction. (*B*) Cartoon depicting the strategy for creating a pore-only channel. Two of the four VSDs are shown along with the S4–S5 linker. Scissors indicate the dissection point (*Left*). (*C*) Superdex 200 size-exclusion chromatography of Na_VSp1p in 200 mM NaCl, 0.3 mM DDM, 20 mM Hepes pH 8.0. (*Inset*) Fifteen percent SDS-PAGE of the peak fraction.

characterization (Fig. 1*A*). Thus, we sought alternative strategies to produce biochemically tractable Na_V samples.

Three lines of evidence have suggested that VGIC members are composed of two domains that can fold independently, the VSD and PD (16–18): comparison of potassium channel gene families (19), structural and chimera studies of potassium channels (16, 20–25), and identification of both pore-only (26) and voltage-sensor-only proteins (27–29). In further support of this idea, the independence of potassium channel PDs have been demonstrated by the functional reconstitution of a PD-only potassium channel from *Listeria monocytogenes* following genetic deletion of the VSD (30). We were inspired by these potassium channel examples and reasoned that the poor size-exclusion chromatography behavior of Na_VSp1 was most likely caused by VSD conformational heterogeneity. Therefore, we decided to execute a protein dissection strategy that would remove the likely problematic region, the VSD, and create a pore-only sodium channel, Na_VSp1p, by cutting the protein in the S4–S5 linker region that connects the VSD to the PD (Fig. 1*B* and Fig. S1*A*). In line with our expectations, the pore-only construct Na_VSp1p was expressed in the membrane fraction of *E. coli* to very high levels as a hexahistidine tag, maltose binding protein fusion (>25 mg L^{-1}), and yielded material that displayed greatly improved size-exclusion behavior relative to full-length Na_VSp1 following removal of the affinity tags and purification (Fig. 1 *A* and *C*). These properties made Na_VSp1p very suitable for further biochemical and biophysical characterization.

Biophysical Characterization Demonstrates That Na_VSp1p Is Folded and Forms Tetramers. Structurally characterized VGIC members have high α-helical content (16, 24, 31, 32). To examine Na_VSp1p secondary structure, we used circular dichroism (CD) and measured spectra in two different detergents, n-dodecyl-β-D-maltopyranoside (DDM) and n-decyl-β-D-maltopyranoside (DM). In both, Na_VSp1p showed the characteristic hallmark double minima of helical proteins (Fig. 2*A*) (33). These spectral signatures are similar to those reported for purified, detergent-solubilized full-length Na_VBh1 (NaChBac) (12, 13), electric eel Na_V (34), and the pore-only potassium channel KcsA (35, 36) and indicate that Na_VSp1p has the high α-helical content characteristic of the VGIC superfamily. Thermal denaturation experiments monitored by CD indicate that Na_VSp1p undergoes a cooperative loss of secondary structure (Fig. 2*B*) that is characteristic of a folded protein and that resembles that seen in the full-length electric eel Na_V (34). Moreover, Na_VSp1p has different degrees of stability in DDM and DM (apparent melting temperatures, Tms, of 44 °C and 52 °C, respectively) and the thermal transition in DDM can be made largely reversible (90% recovery of the signal at 222 nm) by the inclusion of 8% glycerol (Fig. S1*B*). Together, these spectral and thermal denaturation properties suggest that Na_VSp1p is a well-folded, α-helical protein that has similar secondary structure to other members of the VGIC superfamily.

Prior studies of purified full-length Na_VBh1 indicate that bacterial Na_Vs are tetramers (14). We expected that this property should be maintained in Na_VSp1p and used two independent methods to probe Na_VSp1p oligomerization (Table 1): glutaraldehyde (GTA) chemical cross-linking (37, 38) and size-exclusion chromatography coupled with triple detector analysis (SEC-TDA) (39). SDS-PAGE analysis of GTA cross-linked Na_VSp1p solubilized in DDM revealed the presence of three cross-linked products that corresponded to dimers, trimers, and tetramers, but did not indicate higher-order species (Fig. 2*C* and Table 1). Altering the conditions to favor more extensively cross-linked species showed a reduction of lower-order cross-linked species and enhancement of the tetrameric species, thereby indicating that Na_VSp1p assembles into a complex containing four subunits. This behavior was recapitulated in DM (Fig. S1*C*).

We further examined the association state of Na_VSp1p by SEC-TDA. This methodology, in which changes in refractive index, ultraviolet absorption, and static angle light scattering are

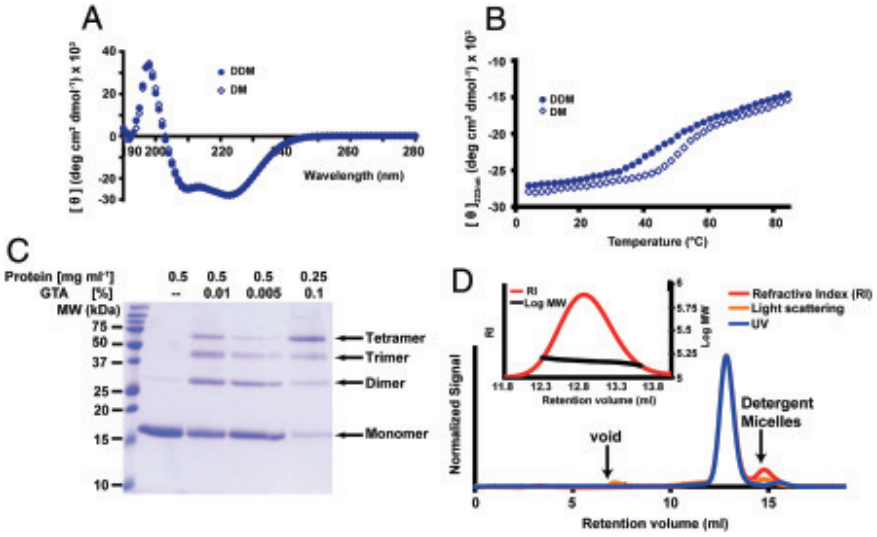

Fig. 2. Biophysical characterization of Na_VSp1p. (*A*) CD spectra for Na_VSp1p at 4 °C in 150 mM NaCl, 10 mM Na-phosphate pH 7.4, and either 0.3 mM DDM or 2.7 mM DM. (*B*) Thermal denaturation of Na_VSp1p in the same buffers as *A*, monitored by CD at 222 nm. (*C*) SDS-PAGE analysis for GTA cross-linked Na_VSp1p in DDM. Protein concentrations, GTA concentrations, and oligomeric species are indicated. (*D*) Na_VSp1p exemplar SEC-TDA in 200 mM NaCl, 0.3 mM DDM, 20 mM Hepes, pH 8.0. Void and empty micelle positions are indicated. (*Inset*) Molecular weight distribution across the main peak.

Table 1. Oligomeric states of pore-only proteins

	GTA cross-linking	SEC-TDA					
	Number of subunits	Number of subunits	Mass, kDa	Mw/Mn	Mw	Monomer mass, kDa	n
Na_VSp1p	4 (DDM) 4 (DM)	4.2 ± 0.1 (DDM)	67.3 ± 1.9	1.057	168.2 ± 0.6	15.87	4
Na_VAb1p	4 (DDM)	4.3 ± 0.1 (DDM)	72.6 ± 2.3	1.004	145.6 ± 2.1	17.27	5
Na_VAe1p	4 (DDM)	4.1 ± 0.2 (DDM)	70.8 ± 3.1	1.015	154.1 ± 4.4	17.45	5
Ca_VSp1p	4 (DM)	4.3 ± 0.1 (DM)	68.8 ± 1.2	1.011	130.1 ± 1.4	15.87	4

measured, allows determination of the absolute molecular weight of the protein component of the protein-detergent micelle (39, 40) and has been recently applied to determine the association states of a variety of membrane proteins in different detergents (41–43). SEC-TDA of Na_VSp1p (Fig. 2*D*) indicates that the protein complex is a monodisperse entity that contains four monomers (Table 1). The excellent agreement between these experiments and the GTA experiments provides strong evidence that Na_VSp1p is a tetramer.

Functional Characterization of Reconstituted Na_VSp1p. Although the biochemical evidence provided strong indications that Na_VSp1p is a folded, tetrameric protein, it was essential to determine whether Na_VSp1p retained any functional ion channel properties. Therefore, we reconstituted purified Na_VSp1p into 1,2-diphytanoyl-sn-glycero-3-phosphocholine (DPhPC) giant unilamellar vesicles (GUVs) created by electroformation (44, 45) and assayed the properties of the reconstituted channels using planar patch clamp technology (46, 47). Measurement of the reversal potential of bilayers containing hundreds of channels under asymmetric NaCl conditions yielded $E_{rev} = 53.69 \pm 8.05$ mV ($n = 6$) (Fig. S2) in good agreement with the expected Nernst potential for sodium, 58.5 mV, and indicated that Na_VSp1p is a cation-selective channel. Following bilayer formation, varying the holding potential between −80 mV and +100 mV revealed channel activity displaying spontaneous openings ($n = 7$, where n is the number of bilayers with activity formed over the glass aperture) (Fig. 3*A*). As expected from the absence of the VSD, Na_VSp1p activity lacked a strong voltage dependence (Fig. 3*B* and Fig. S3). Importantly, application of mibefradil, a Ca_V blocker that blocks bacterial Na_Vs (9, 13), inhibited the activity of the purified, reconstituted Na_VSp1p (Fig. 3 *C* and *D*) and provided evidence that the ion channel activity was the result of a reconstituted sodium channel.

To characterize the biophysical properties of the Na_VSp1p channel further, we measured its ion selectivity properties. Comparison of the selectivity for sodium, potassium, and calcium ions by measuring the reversal potentials in a set of asymmetric ion conditions indicated that Na_VSp1p has a preference for permeant ions of $Na^+:K^+:Ca^{2+} = 1:0.22:0.08$ (Fig. 3 *B* and *E* and Table 2). The measured preference for sodium over calcium ($P_{Ca}/P_{Na} = 0.08$) is in good agreement with the reported value for the related bacterial channel Na_VBh1 ($P_{Ca}/P_{Na} = 0.15$) (10), which bears strong similarity to Na_VSp1p in the selectivity filter (Fig. 4*A* and Fig. S1*A*). These selectivity properties, together with the sensitivity to mibefradil, indicate that the core functions of the PD, ion selectivity and conduction, remain intact and provide strong evidence that the folded, tetrameric Na_VSp1p forms a functional, stand-alone ion selective channel.

Selectivity Filter Mutations Convert Na_VSp1p into a Calcium-Selective Channel, Ca_VSp1p. It has long been thought that the selectivity filters of Na_Vs and Ca_Vs are related (4). In accord with this view, bacterial Na_Vs bear sequence similarity to both Na_Vs and Ca_Vs (9). Further, prior studies of bacterial Na_V selectivity filter elements have shown that a triple aspartate mutation in the Na_VBh1 (NaChBac) selectivity filter amino acid sequence, LESWAS → LDDWAD, creates a channel Ca_VBh1 ($CaChBac_m$) that is calcium-selective rather than sodium-selective (10). We incorporated the same triple aspartate change into the analogous Na_VSp1p selectivity filter positions to create a mutant channel "Ca_VSp1p" (Fig. 4*A*). Characterization of purified Ca_VSp1p by CD, GTA cross-linking, and SEC-TDA (Fig. 4 *B–D* and Table 1) showed that Ca_VSp1p had physical properties that were identical to Na_VSp1p. Importantly, incorporation of Ca_VSp1p into DPhPC GUVs and subsequent electrophysiological recording by planar patch clamp revealed that Ca_VSp1p forms functional channels (Fig. 4 *E* and *F*). In stark contrast to Na_VSp1p, Ca_VSp1p channels were calcium-selective (Fig. 4*G* and Table 2) and displayed an approximately 30-fold increase in single channel conductance in calcium compared to Na_VSp1p (335.3 ± 6.2 pS versus 31.1 ± 1.4 pS, for Ca_VSp1p and Na_VSp1p, respectively, Table 2) and approximately 39-fold change in P_{Ca}/P_{Na} (3.13 ± 0.16 versus 0.08 ± 0.01 for Ca_VSp1p and Na_VSp1p, respectively, Table 2).

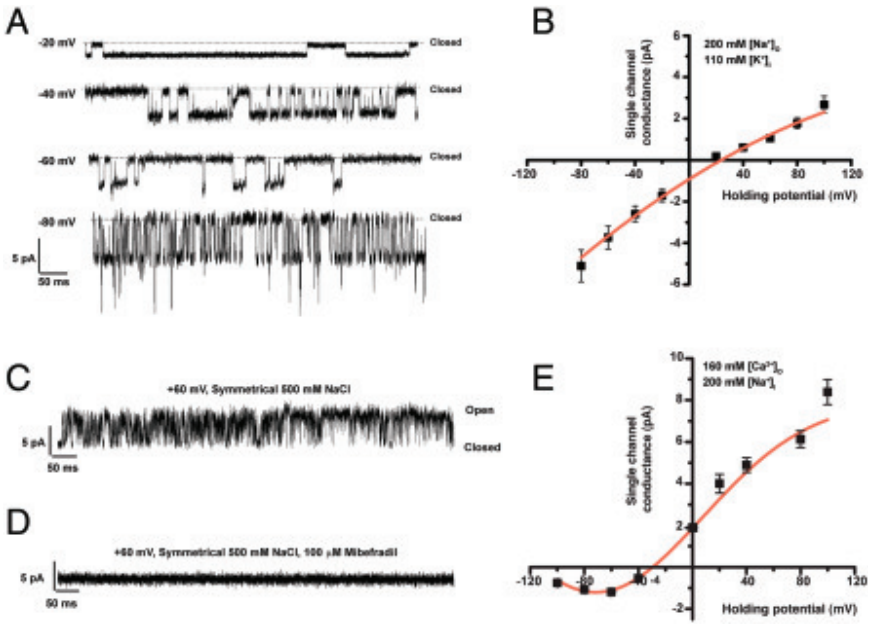

Fig. 3. Electrophysiological characterization of reconstituted Na_VSp1p. (*A*) Representative traces recorded from a planar lipid bilayer containing single Na_VSp1p channels at the indicated holding potentials using 110 mM KCl, 10 mM Hepes, pH 7.0 and 200 mM NaCl, 10 mM Hepes, pH 7.0 internal and external solutions, respectively. Closed channel current level is indicated. (*B*) Single channel *I–V* relationships for Na_VSp1p channels in 110 mM KCl internal, $[K^+]_I$, and NaCl 200 mM external, $[Na^+]_O$, solutions. (*C* and *D*) Bilayer recordings of Na_VSp1p at +60 mV in symmetrical 500 mM NaCl before (*C*) and after (*D*) addition of 100 μM mibefradil. (*E*) Single channel *I–V* relationships for Na_VSp1p channels in 200 mM NaCl internal, $[Na^+]_I$ and 160 mM $CaCl_2$ external, $[Ca^{2+}]_O$, solutions. *I–V* curves in *B* and *E* are derived from single channel recordings of multiple bilayers.

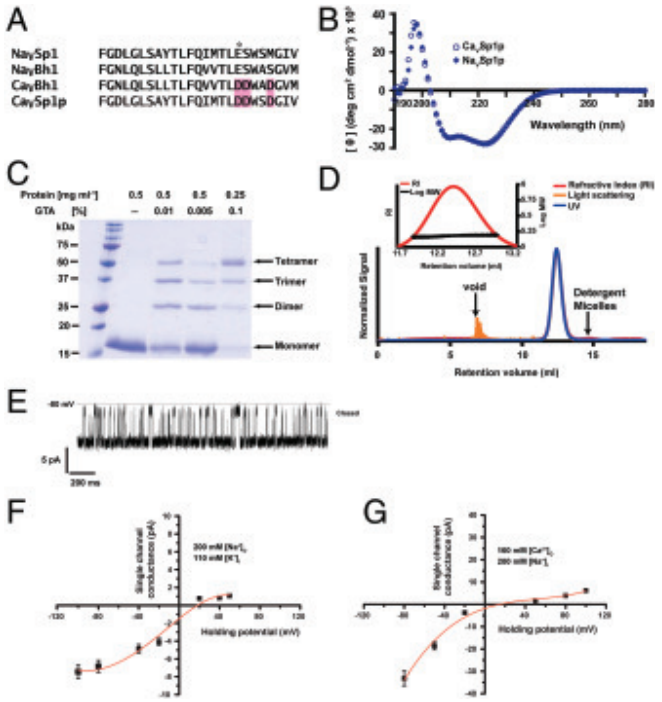

Fig. 4. Characterization of a calcium-selective Na_VSp1p mutant. (*A*) Pore region sequence comparison. Residues changed to alter Ca_VBh1 and Ca_VSp1p ion selectivity are highlighted. (*B*) Comparison of Ca_VSp1p (open circles) and Na_VSp1p (blue circles) CD spectra at 4 °C in 150 mM NaCl, 2.7 mM DM, 10 mM naphosphate, pH 7.4. (*C*) SDS-PAGE analysis for GTA cross-linked Ca_VSp1p in DM. Protein concentrations, GTA concentrations, and oligomeric species are indicated. (*D*) Ca_VSp1p exemplar SEC-TDA in 200 mM NaCl, 2.7 mM DM, 20 mM Hepes, pH 8.0. Void and empty micelle positions are indicated. (*Inset*) Molecular weight distribution across the main peak. (*E*) Representative trace at −80 mV holding potential from a planar lipid bilayer containing Ca_VSp1p using 200 mM NaCl, 10 mM Hepes, pH 7.0; and 110 mM KCl, 10 mM Hepes, pH 7.0 external and internal solutions, respectively. Closed channel current level is indicated. (*F*) Single channel *I–V* relationships for Ca_VSp1p in the solutions from *E* indicated as $[K^+]_I$ internal and $[Na^+]_O$ external. Solid line was obtained by a nonlinear fit. (*G*) Single channel current voltage relationships for Ca_VSp1p channels measured using 200 mM NaCl internal, $[Na^+]_I$ and 160 mM $CaCl_2$ external, $[Ca^{2+}]_O$, solutions. Solid line was obtained by a nonlinear fit.

These data are consistent with the previous studies of Ca_VBh1 (10) and show definitively that the measured single channel currents must arise from the reconstituted channels.

Generation of Pore-Only Proteins from Other Extremophile Na_Vs. To test whether the ability to make folded PDs could be generalized to other Na_Vs, we investigated the application of the dissection approach to three related extremophile bacterial Na_Vs. To examine a diverse set, we picked Na_Vs that have sequence identities of approximately 50% or less with Na_VSp1p. These included the well-characterized *Bacillus halodurans* Na_VBh1 (NaChBac) (9) (40% identical to Na_VSp1p), an Na_V from the hydrocarbon degrading bacterium *Alcanivorax borkumensis* (51% identical to Na_VSp1p), and the Na_V from the arsenite oxidizing bacterium *Alkalilimnicola ehrlichei* (48% identical to Na_VSp1p), (Fig. 5 *A* and *B* and Fig. S1*A*). Attempts to purify Na_VBh1p were unsuccessful. However, we were able to express, purify, and characterize pore-only proteins from Na_VAb1 and Na_VAe1. Both showed CD spectra that were very similar to that of Na_VSp1p (Fig. 6 *A* and *B*). Additionally, GTA cross-linking (Fig. 6 *C* and *D*) and SEC-TDA analysis (Fig. 6 *E* and *F*) indicated that Na_VAb1p and Na_VAe1p form tetramers. Further, reconstitution of Na_VAb1p into GUVs and measurement by planar patch clamp methodology revealed the activity of single channels lacking a strong voltage dependence (Fig. 6 *G* and *H* and Fig. S3) and having a single channel conductance very similar to that of Na_VSp1p, 37.3 ± 1.5 pS. Interestingly, Na_VAb1p has different behavior than Na_VSp1p and displays a lower open probability (e.g., Po at +80 mV of 0.5 versus 0.25 for Na_VSp1p and Na_VAb1p, respectively, Fig. S3) but substantially longer channel openings. These differences must arise from divergent elements in the PDs that affect the intrinsic properties of the PD. Similar functional studies with Na_VAe1p did not yield clear single channel activity and were not analyzed further. Taken together, the similarity of the biophysical properties of Na_VAb1p and Na_VAe1p to Na_VSp1p demonstrate that Na_VAb1p and Na_VAe1p are well-folded, stand-alone pore domains. These results show that the protein dissection approach to create PD-only proteins can be generalized and should be applicable to a range of VGICs.

Table 2. Ion conduction and selectivity properties for Na_VSp1p and LDDWSD mutant Ca_VSp1p

Pore sequence		Ion	Conductance, pS	G_x/G_{Na+}	P_x/P_{Na^+}
Na_VSp1p	FQIMT*LESWSM*GIV	Na^+	31.1 ± 1.4	1	1
		K^+	18.4 ± 2.1	0.59	0.22 ± 0.01
		Ca^{2+}	10.7 ± 1.7	0.34	0.08 ± 0.01
Ca_VSp1p	FQIMT*LDDWSD*GIV	Na^+	74.4 ± 4.2	1	1
		K^+	30.3 ± 2.9	0.41	0.25 ± 0.01
		Ca^{2+}	335.3 ± 6.2	4.51	3.13 ± 0.16

$n = 7$ except for Ca_VSp1p P_{K^+}/P_{Na^+} where $n = 5$. Values are mean ± SD. Ratios were measured using 200 mM NaCl, 110 mM KCl, and 160 mM $CaCl_2$.

Discussion

Developing a detailed understanding of the structural principles that underlie VGIC superfamily transmembrane architecture is an important goal that has a direct bearing on elaboration of channel gating and ion permeation mechanisms, design of ion channels having unique function, drug development, and understanding channel evolution. Within the VGIC superfamily, a number of lines of evidence have suggested that the transmembrane segments of K_V channels are arranged in distinct domains comprising the VSD and PD. This possibility was first noted from comparison of K_V channels, which have six-transmembrane segments that include a VSD, and inward rectifiers, which contain only a two-transmembrane pore-forming unit, as both contain common pore elements (19). A variety of structural and chimera studies of different potassium channels have further supported this intramembrane domain segregation idea (16, 20–25). Most notably, independent X-ray and NMR structures of the VSD from the *Aeropyrum pernix* voltage-gated potassium channel KvAP show that the VSD can fold separately from the pore domain (23, 25); however, this folding appears to be subject to strong context-dependent effects (23, 48). Additional evidence for potassium channel transmembrane modularity comes from the recent purification and reconstitution of a PD-only potassium channel from *Listeria monocytogenes* following genetic removal of the VSD (30). Besides these potassium channel studies, the idea

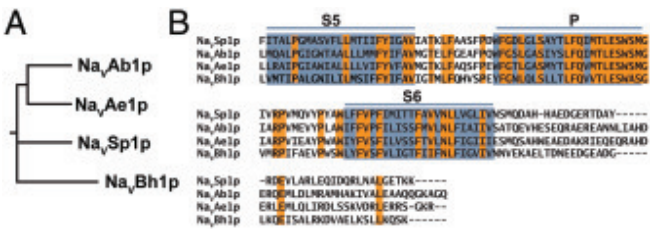

Fig. 5. Sequence relationships of bacterial Na_Vs. (*A*) Phylogenetic tree of the pore regions of from *A. borkumensis* (Na_VAb1p), *A. ehrlichei* (Na_VAe1p), *S. pomeroyi* (Na_VSp1p), and *B. halodurans* (Na_VBh1p). (*B*) Sequence alignment of Na_VAb1p, Na_VAe1p, Na_VSp1p, and Na_VBh1p. Absolutely conserved residues are shown in orange. Blue shading and lines indicate the predicted transmembrane segments S5 and S6 and the pore region, P.

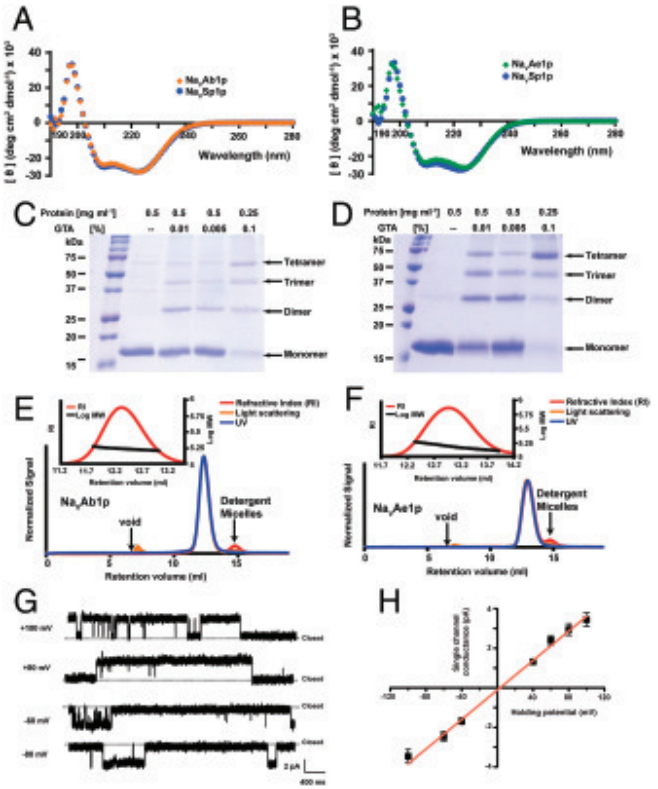

Fig. 6. Na_VAb1p and Na_VAe1p characterization. Comparison of CD spectra of *A*, Na_VAb1p (orange diamonds) and *B*, Na_VAe1p (green diamonds) with Na_VSp1p (blue circles) at 4 °C in 150 mM NaCl, 0.3 mM DDM, 10 mM naphosphate, pH 7.4; 15% SDS-PAGE analysis for GTA cross-linked (*C*) Na_VAb1p and (*D*) Na_VAe1p in DDM. Protein concentrations, GTA concentrations, and oligomeric species are indicated; exemplar SEC-TDA of (*E*) Na_VAb1p and (*F*) Na_VAe1p in 200 mM NaCl, 0.3 mM DDM, 20 mM Hepes, pH 8.0. Void and empty detergent micelles positions are indicated. (*Inset*) Molecular weight distribution across the main peak. (*G*) Representative traces recorded from a planar lipid bilayer containing Na_VAb1p at different holding potentials as indicated using symmetrical 200 mM NaCl, 10 mM Hepes, pH 7.0. (*H*) Na_VAb1p single channel current–voltage relationships. Main conductance was calculated from the slope of the linear regression and was 37.3 ± 1.5 pS.

that the VSD can fold and function independently from the PD (17, 18) has been further advanced by the identification of a family of voltage-sensor-only proteins (27–29). Nevertheless, despite this accumulating evidence, whether this principle of modular transmembrane structural arrangement exists in other members of the VGIC family has remained untested. Further, to date, no naturally occurring PD-only channels from the Na_V, Ca_V, or TRP branches of the VGIC superfamily have been reported.

Our data demonstrate that transmembrane structural modularity is present in members of the Na_V family. We show that it is possible to generate pore-domain-only proteins from three different extremophile Na_Vs by genetic excision of the VSD: *S. pomeroyi*, Na_VSp1p, *A. borkumensis*, Na_VAb1p, and *A. ehrlichei*, Na_VAe1p. In all cases, the PDs can be expressed in the *E. coli* membrane fraction in amounts that facilitate purification and characterization (approximately 25 $mg\,L^{-1}$). Further, all three PDs form stable, tetrameric complexes in at least one mild detergent, either DDM or DM. Importantly, both Na_VSp1p and Na_VAb1p form functional ion channels when reconstituted into lipid bilayers. Critically, electrophysiological studies of purified Na_VSp1p reconstituted into lipid bilayers demonstrate that Na_VSp1p retains the principal properties of a bacterial sodium channel. Na_VSp1p forms ion channels having a selectivity sequence of $Na^+:K^+:Ca^{2+} = 1:0.22:0.08$ (Table 2) and is sensitive to block by a known bacterial Na_V pore blocker, mibefradil (9, 13) (Fig. 3 *C* and *D*). Taken together, these data strongly indicate that the pore-only proteins are folded properly and retain the core functions of the pore domain, which are to act as functional ion channels that maintain ion selectivity.

Functional studies of a number of bacterial Na_Vs have shown them to be sodium-selective (8–10). Yet, in line with the close evolutionary relationship of Na_Vs and Ca_Vs (1–4), the bacterial Na_V selectivity filter sequences also bear some sequence similarity to those of Ca_Vs (9, 10, 49). Incorporation of a triple aspartate change in the Na_VBh1p (NaChBac) selectivity filter sequence, LESWAS → LDDWAD, turns Na_VBh1p from a sodium-selective channel into a calcium-selective channel, Ca_VBh1 ($CaChBac_m$) (10). Our data show that incorporation of the analogous aspartate triple mutant into the Na_VSp1p selectivity filter creates a calcium-selective channel, Ca_VSp1p (Fig. 4*G* and Table 2). Similar to Ca_VBh1 ($CaChBac_m$) (10) Ca_VSp1p not only prefers calcium over sodium but also retains a preference for sodium over potassium (Table 2). The creation of the calcium-selective channel Ca_VSp1p together with the three pore-only Na_Vs we describe establishes a set of biochemically tractable proteins that should allow the exploration of the atomic basis for both sodium and calcium selectivity.

The complexity and transmembrane nature of VGIC superfamily members remains a barrier to understanding their function from a high-resolution structural standpoint. The demonstration that it is generally feasible to create folded and functional PDs from a variety of extremophile Na_Vs, including channels that are either sodium- or calcium-selective, opens the possibility that this strategy may lead to the crystallization and structure determination of both sodium- and calcium-selective pores. Further, the biochemical tractability of the PD-only proteins may permit them to be used as platforms for screening and characterization of previously undescribed peptide or small molecule pore blockers.

The PDs display an apparent general conformational and functional robustness that contrasts with the context-dependent folding and conformational heterogeneity of the VSD. Such robustness is consistent with the high stereochemical demands required to make a channel that is selective for particular permeant ions. The independent folding of PDs as demonstrated here for Na_Vs and by Montal and colleagues for K_Vs (50) suggests that similar strategies may be applicable for other members of the VGIC superfamily. Such efforts may facilitate attempts to obtain structural information about the pore regions of homomeric members of the VGIC that presently lack structural data such as TRP channels.

Taken together with the previous work on potassium channels (16, 20–26) and voltage-sensor only proteins (27–29), our results provide support for the general independent nature of the PD and VSD within the VGIC superfamily. This concept is also supported by recent studies from McCusker et al. that reported the creation of an Na_VSp1 pore-only protein (51) similar to the one described here. This modular division is consistent with the hypothesis that the architecture of the transmembrane parts of the VGIC reflects an evolutionary path where various types of sensor domains were fused to a core, pore-forming module to generate a diversity of gating responses (19).

Materials and Methods

Molecular Biology and Protein Purification. Please see *SI Text* for a detailed description of the molecular biology and purification methods used to make the described Na_V PDs.

Circular Dichroism Spectroscopy. CD spectra were recorded on an Aviv 215 circular dichroism spectrometer using a 1-mm path-length quartz cell at 4 °C. Melting temperature, Tm, was determined as the inflection point of first derivative of the data.

Cross-Linking. Purified pore proteins, 10 μg or 5 μg, were combined with 0.01% and 0.005% or 0.1% glutaraldehyde (Aldrich), respectively, in a final volume of 20 μL and incubated for 10 min at 37 °C. Reactions were quenched

with a final concentration of 100 mM Tris pH 8.0 at room temperature and boiled for 10 min in a reducing SDS-sample buffer prior to analysis by 15% SDS-PAGE and Coomassie brilliant blue R-250.

Size-Exclusion Chromatography–Tridetector Analysis. Simultaneous detection of UV, refractive index, and right angle light scattering signals from SEC of pore-only domains was performed using a Viscotek 302 Tetra Detector Array (TDA, Malvern/Viscotek) in line with a Superdex 200 10/300 GL (GE Healthcare) column.

Functional Characterization of Reconstituted Pore-Only Proteins. Lipid bilayer experiments performed using a planar patch clamp system (Port-a-Patch, Nanion Technologies GmbH) on Na_VSp1p, Na_VAe1p, or Na_VAb1p were incorporated into GUVs using procedures described previously (44, 45). To determine Na^+, K^+, and Ca^{2+} permeabilities, the reversal potential was measured in asymmetric conditions where the internal solution contained 10 mM Na-Hepes, 200 mM NaCl, pH 7.0 (adjusted with NaOH) and the external solution contained 10 mM Hepes, 160 mM $CaCl_2$, pH 7.0 (adjusted with HCl) or 10 mM Hepes, 110 mM KCl, pH 7.0 (adjusted with KOH). The permeability ratio of ions was estimated according to the following equation: $P_{Na}/P_x = a_{si}[\exp(E_{rev}F/RT)][\exp(E_{rev}F/RT)+1]/(4a_{se})$ (10). R, T, F, and E_{rev} are the gas constant, absolute temperature, Faraday constant, and treversal potential, respectively; "x" represents K^+ or Ca^{2+}. Activity coefficients for Na^+, K^+, and Ca^{2+} were estimated as follows: $a_s = \gamma_s[X_s]$, where activity, a_s, is the effective concentration of an ion in solution, s is related to the nominal concentration $[X_s]$ by the activity coefficient, γ_s, γ_s was calculated from the Debye–Hückel equation: $\log\gamma_s = -0.51 * z_s\sqrt[2]{\mu}/(1+3.8\alpha_s\sqrt{\mu})$, where μ is the ionic strength of the solution, z_s is the charge on the ion, and α_s is the effective diameter of the hydrated ion in nanometers.

Detailed procedures can be found in *SI Text*.

ACKNOWLEDGMENTS. We thank L. Ma, A. Moroni, E. Reuveny, and G. Thiel for comments and Minor lab members for support. This work was supported by National Institutes of Health Grants R01-HL080050, R01-DC007664, and U54GM094625 (to D.L.M.) and the American Heart Association (AHA) Grant 0740019N (to D.L.M.). R.A.R. was supported by P50-GM73210. D.L.M. is an AHA Established Investigator.

1. Yu FH, Catterall WA (2004) The VGL-chanome: A protein superfamily specialized for electrical signaling and ionic homeostasis. *Sci STKE* 2004:re15.
2. Yu FH, Yarov-Yarovoy V, Gutman GA, Catterall WA (2005) Overview of molecular relationships in the voltage-gated ion channel superfamily. *Pharmacol Rev* 57:387–395.
3. Goldin AL (2002) Evolution of voltage-gated $Na^{(+)}$ channels. *J Exp Biol* 205:575–584.
4. Hille B (2001) *Ion Channels of Excitable Membranes* (Sinauer Associates, Inc, Sunderland, MA), 3rd Ed.
5. Bhattacharya A, Wickenden AD, Chaplan SR (2009) Sodium channel blockers for the treatment of neuropathic pain. *Neurotherapeutics* 6:663–678.
6. England S, de Groot MJ (2009) Subtype-selective targeting of voltage-gated sodium channels. *Br J Pharmacol* 158:1413–1425.
7. Perret D, Luo ZD (2009) Targeting voltage-gated calcium channels for neuropathic pain management. *Neurotherapeutics* 6:679–692.
8. Koishi R, et al. (2004) A superfamily of voltage-gated sodium channels in bacteria. *J Biol Chem* 279:9532–9538.
9. Ren D, et al. (2001) A prokaryotic voltage-gated sodium channel. *Science* 294:2372–2375.
10. Yue L, Navarro B, Ren D, Ramos A, Clapham DE (2002) The cation selectivity filter of the bacterial sodium channel, NaChBac. *J Gen Physiol* 120:845–853.
11. Sato C, et al. (2001) The voltage-sensitive sodium channel is a bell-shaped molecule with several cavities. *Nature* 409:1047–1051.
12. O'Reilly AO, Charalambous K, Nurani G, Powl AM, Wallace BA (2008) G219S mutagenesis as a means of stabilizing conformational flexibility in the bacterial sodium channel NaChBac. *Mol Membr Biol* 25:670–676.
13. Nurani G, et al. (2008) Tetrameric bacterial sodium channels: Characterization of structure, stability, and drug binding. *Biochemistry* 47:8114–8121.
14. Mio K, Mio M, Arisaka F, Sato M, Sato C (2010) The C-terminal coiled-coil of the bacterial voltage-gated sodium channel NaChBac is not essential for tetramer formation, but stabilizes subunit-to-subunit interactions. *Prog Biophys Mol Biol* 103:111–121.
15. Hammon J, Palanivelu DV, Chen J, Patel C, Minor DL, Jr (2009) A green fluorescent protein screen for identification of well-expressed membrane proteins from a cohort of extremophilic organisms. *Protein Sci* 18:121–133.
16. Long SB, Campbell EB, Mackinnon R (2005) Crystal structure of a mammalian voltage-dependent Shaker family K^+ channel. *Science* 309:897–903.
17. Minor DL, Jr (2006) A sensitive channel family replete with sense and motion. *Nat Struct Mol Biol* 13:388–390.
18. Okamura Y, Murata Y, Iwasaki H (2009) Voltage-sensing phosphatase: actions and potentials. *J Physiol* 587:513–520.
19. Jan LY, Jan YN (1994) Potassium channels and their evolving gates. *Nature* 371:119–122.
20. Caprini M, et al. (2001) Structural compatibility between the putative voltage sensor of voltage-gated K^+ channels and the prokaryotic KcsA channel. *J Biol Chem* 276:21070–21076.
21. Lu Z, Klem AM, Ramu Y (2001) Ion conduction pore is conserved among potassium channels. *Nature* 413:809–813.
22. Lu Z, Klem AM, Ramu Y (2002) Coupling between voltage sensors and activation gate in voltage-gated K^+ channels. *J Gen Physiol* 120:663–676.
23. Jiang Y, et al. (2003) X-ray structure of a voltage-dependent K^+ channel. *Nature* 423:33–41.
24. Long SB, Tao X, Campbell EB, MacKinnon R (2007) Atomic structure of a voltage-dependent K^+ channel in a lipid membrane-like environment. *Nature* 450:376–382.
25. Butterwick JA, MacKinnon R (2010) Solution structure and phospholipid interactions of the isolated voltage-sensor domain from KvAP. *J Mol Biol* 403:591–606.
26. Plugge B, et al. (2000) A potassium channel protein encoded by chlorella virus PBCV-1. *Science* 287:1641–1644.
27. Murata Y, Iwasaki H, Sasaki M, Inaba K, Okamura Y (2005) Phosphoinositide phosphatase activity coupled to an intrinsic voltage sensor. *Nature* 435:1239–1243.
28. Ramsey IS, Moran MM, Chong JA, Clapham DE (2006) A voltage-gated proton-selective channel lacking the pore domain. *Nature* 440:1213–1216.
29. Sasaki M, Takagi M, Okamura Y (2006) A voltage sensor-domain protein is a voltage-gated proton channel. *Science* 312:589–592.
30. Santos JS, Grigoriev SM, Montal M (2008) Molecular template for a voltage sensor in a novel K^+ channel. III. Functional reconstitution of a sensorless pore module from a prokaryotic Kv channel. *J Gen Physiol* 132:651–666.
31. Doyle DA, et al. (1998) The structure of the potassium channel: Molecular basis of K^+ conduction and selectivity. *Science* 280:69–77.
32. Jiang Y, et al. (2002) Crystal structure and mechanism of a calcium-gated potassium channel. *Nature* 417:515–522.
33. Berova N, Nakanishi K, Woody RW (2000) *Circular Dichroism: Principles and Applications* (Wiley-VCH, New York), 2nd Ed.
34. Charalambous K, O'Reilly AO, Bullough PA, Wallace BA (2009) Thermal and chemical unfolding and refolding of a eukaryotic sodium channel. *Biochim Biophys Acta* 1788:1279–1286.
35. Chill JH, Louis JM, Delaglio F, Bax A (2007) Local and global structure of the monomeric subunit of the potassium channel KcsA probed by NMR. *Biochim Biophys Acta* 1768:3260–3270.
36. Barrera FN, et al. (2005) Unfolding and refolding in vitro of a tetrameric, alpha-helical membrane protein: The prokaryotic potassium channel KcsA. *Biochemistry* 44:14344–14352.
37. Maduke M, Pheasant DJ, Miller C (1999) High-level expression, functional reconstitution, and quaternary structure of a prokaryotic ClC-type chloride channel. *J Gen Physiol* 114:713–722.
38. Robertson JL, Kolmakova-Partensky L, Miller C (2010) Design, function and structure of a monomeric ClC transporter. *Nature* 468:844–847.
39. Slotboom DJ, Duurkens RH, Olieman K, Erkens GB (2008) Static light scattering to characterize membrane proteins in detergent solution. *Methods* 46:73–82.
40. Hayashi Y, Matsui H, Takagi T (1989) Membrane protein molecular weight determined by low-angle laser light-scattering photometry coupled with high-performance gel chromatography. *Methods Enzymol* 172:514–528.
41. Dorwart MR, Wray R, Brautigam CA, Jiang Y, Blount P (2010) S. aureus MscL is a pentamer in vivo but of variable stoichiometries in vitro: implications for detergent-solubilized membrane proteins. *PLoS Biol* 8:e1000555.
42. Waight AB, Love J, Wang DN (2010) Structure and mechanism of a pentameric formate channel. *Nat Struct Mol Biol* 17:31–37.
43. ter Beek J, Duurkens RH, Erkens GB, Slotboom DJ (2011) Quaternary structure and functional unit of energy coupling factor (ECF)-type transporters. *J Biol Chem* 286:5471–5475.
44. Kreir M, Farre C, Beckler M, George M, Fertig N (2008) Rapid screening of membrane protein activity: Electrophysiological analysis of OmpF reconstituted in proteoliposomes. *Lab Chip* 8:587–595.
45. Gassmann O, et al. (2009) The M34A mutant of Connexin26 reveals active conductance states in pore-suspending membranes. *J Struct Biol* 168:168–176.
46. Farre C, et al. (2009) Port-a-patch and patchliner: High fidelity electrophysiology for secondary screening and safety pharmacology. *Comb Chem High Throughput Screen* 12:24–37.
47. Behrends JC, Fertig N (2007) Planar patch clamping. *Patch-Clamp Analysis: Advanced Techniques*, Neuromethods, ed W Walz (Humana Press, Totowa, NJ), 2nd Ed, Vol 38,, pp 441–433.
48. Lee SY, Lee A, Chen J, MacKinnon R (2005) Structure of the KvAP voltage-dependent K^+ channel and its dependence on the lipid membrane. *Proc Natl Acad Sci USA* 102:15441–15446.
49. Durell SR, Guy HR (2001) A putative prokaryote voltage-gated $Ca^{(2+)}$ channel with only one 6TM motif per subunit. *Biochem Biophys Res Commun* 281:741–746.
50. Santos JS, Lundby A, Zazueta C, Montal M (2006) Molecular template for a voltage sensor in a novel K^+ channel. I. Identification and functional characterization of KvLm, a voltage-gated K^+ channel from Listeria monocytogenes. *J Gen Physiol* 128:283–292.
51. McCusker EC, D'Avanzo N, Nichols CG, Wallace BA (2011) A simplified bacterial "Pore" provides insight into the assembly, stability and structure of sodium channels. *J Biol Chem* 286:16386–16391.